

Line Start Permanent Magnet Motor: Single-Phase Starting Performance Analysis

M. Popescu T.J.E. Miller M.I. McGilp
SPEED Laboratory, University of Glasgow,
Oakfield Avenue, Rankine Building,
Glasgow G12 8LT - UNITED KINGDOM

G. Strappazon*) N. Trivillin*) R. Santarossa*)
) Electrolux Compressors,
Via Consorziale, 13 - Comina
33170 Pordenone - ITALY

Abstract This paper presents a detailed quasi steady-state approach to different torque components (average and pulsating) for a single-phase capacitor-run permanent magnet motor. By employing average electromagnetic torque, and the expected envelope of the pulsating torque, an accurate prediction of starting torque components behaviour is made. The quasi steady-state analysis of the asynchronous performance of the single-phase capacitor-start, capacitor-run permanent magnet motor is realized through a combination of symmetrical components and d-q axes theory. The developed approach is valid for any m -phase AC motor – induction, synchronous reluctance or synchronous permanent magnet.

1. INTRODUCTION

Permanent magnet motors, equipped with a cage rotor, may represent a higher-efficiency alternative to induction motors. Generally defined as line-start permanent magnet motors (LSPM), they may be supplied from a three-phase or single-phase voltage system.

LSPM motors run synchronously and this way the cage rotor losses are minimized at nominal load. The capacitor-start, capacitor-run permanent magnet is the single-phase version of the LSPM. This special electrical motor is mainly employed in home appliances, such as refrigerator compressors.

Beneficially for steady-state operation, permanent magnets considerably affect the starting capabilities of such motors. The torque oscillations, during the starting transient, are much higher than for an induction motor.

A detailed approach to different torque components (average and pulsating) for a single-phase capacitor-run permanent magnet motor permits a correct estimation of motor performance. It extends the existent analysis made for a single-phase unsymmetrical [1], [4] or three-phase symmetrical [2], [3] permanent magnet motor. The subject of the analysis for the LSPM motor single-phase starting performance is made over a single-phase capacitor-start, capacitor-run, 50 Hz two-pole motor with concentric windings. The rotor consists of an aluminium rotor cage, with interior ferrite magnets, Fig. 1.

2. MODELLING THE CAGE TORQUES

The traditional way to study the starting process of a LSPM motor is to subdivide it into two different regions [3]:
1- the run-up response up to the “rated induction motor”;
2- the transition zone from that point to synchronism.
The accelerating torque is given by the cage torque minus the magnet braking torque and load torque.

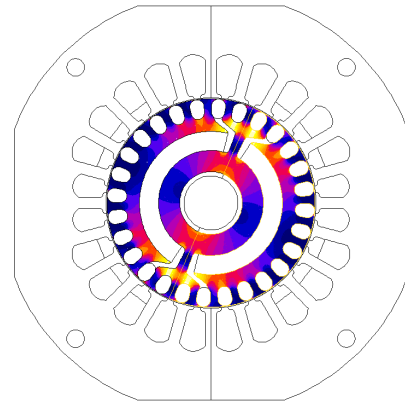


Fig. 1 Cross-section of analysed motor

The unbalanced stator voltage for the case of capacitor start and/or run motors determines different performance for a LSPM motor. It will affect both the starting and steady-state operation of the motor. For a detailed analysis of the torque behaviour of the LSPM motor, a suitable combination of the symmetrical components and d-q axis theory will give accurate results.

An unbalanced supply voltage system can be decomposed using symmetrical components as:

$$\begin{cases} \underline{V}_d = \frac{1}{\sqrt{2}} \cdot (\underline{V}_+ + \underline{V}_-) = \frac{1}{\sqrt{2}} \cdot (\underline{V}_{d+} + \underline{V}_{d-}) \\ \underline{V}_q = \frac{1}{\sqrt{2}} \cdot (-j\underline{V}_+ + j\underline{V}_-) = \frac{1}{\sqrt{2}} \cdot (\underline{V}_{q+} + \underline{V}_{q-}) \end{cases} \quad (1)$$

The positive sequence V_+ will induce currents in the cage rotor of the LSPM motor. The currents frequency will be sf . In a similar way, the negative sequence V_- will induce currents in the cage rotor, with $(2-s)f$ frequency. In double revolving field theory, currents with sf frequency determine the forward field, and the $(2-s)f$ frequency currents determine the backward field. Thus, the initial unbalanced LSPM motor is equivalent to two stator-balanced motors. Each of these fictive motors is characterised by an asymmetrical rotor configuration, due to the cage and the permanent magnets. Using the d-q axis fixed on the rotor frame, we can write the following stator voltage equations for the positive sequence motor:

$$\begin{cases} \underline{V}_{d+} = \underline{V}_+ = R_s \underline{I}_{d+} + js\omega \underline{\psi}_{d+} - (1-s)\omega \underline{\psi}_{q+} \\ \underline{V}_{q+} = -j\underline{V}_+ = R_s \underline{I}_{q+} + js\omega \underline{\psi}_{q+} + (1-s)\omega \underline{\psi}_{d+} \end{cases} \quad (2)$$

and for the negative sequence motor:

$$\begin{aligned} \underline{V}_{d-} = \underline{V}_- &= R_s \underline{I}_{d-} + j(2-s)\omega \underline{\Psi}_{d-} - (1-s)\omega \underline{\Psi}_{q-} \\ \underline{V}_{q-} = j\underline{V}_- &= R_s \underline{I}_{q-} + j(2-s)\omega \underline{\Psi}_{q-} + (1-s)\omega \underline{\Psi}_{d-} \end{aligned} \quad (3)$$

For the flux linkage components we will use the notations [3]:

$$\begin{aligned} \omega \underline{\Psi}_{d\pm} &= \underline{X}_{d\pm} (js) \underline{I}_{d\pm} = -j \underline{Z}_{d\pm} \underline{I}_{d\pm} \\ \omega \underline{\Psi}_{q\pm} &= \underline{X}_{q\pm} (js) \underline{I}_{q\pm} = -j \underline{Z}_{q\pm} \underline{I}_{q\pm} \end{aligned} \quad (4)$$

Introducing (5) in (3) and (4), and solving the equation systems, we obtain the equivalent relations for d-q axis currents:

Positive sequence:

$$\begin{aligned} \underline{I}_{d+} &= \frac{j\underline{V}_+}{D_+} \cdot [-R_s + j(2s-1)\underline{X}_{q+}] \\ \underline{I}_{q+} &= -\frac{\underline{V}_+}{D_+} \cdot [-R_s + j(2s-1)\underline{X}_{d+}] \end{aligned} \quad (5)$$

Negative sequence:

$$\begin{aligned} \underline{I}_{d-} &= \frac{\underline{V}_-}{D_-} \cdot [R_s + j(3-2s)\underline{X}_{d-}] \\ \underline{I}_{q-} &= \frac{j\underline{V}_-}{D_-} \cdot [R_s + j(3-2s)\underline{X}_{q-}] \end{aligned} \quad (6)$$

where:

$$D_+ = R_s^2 + (1-2s)\underline{X}_{d+}\underline{X}_{q+} + jsR_s(\underline{X}_{d+} + \underline{X}_{q+}) \quad (7)$$

$$D_- = R_s^2 + (2s-3)\underline{X}_{d-}\underline{X}_{q-} + j(2-s)R_s(\underline{X}_{d-} + \underline{X}_{q-}) \quad (8)$$

For the single-phase motor, with an unsymmetrical stator winding, by using the relations in [1], we can deduce (the stator windings are assumed to have the same weight, i.e. $R_s = R_m = \beta^2 R_a$, $X_{ls} = X_{lm} = \beta^2 X_{la}$, $\phi_a = \beta^{1/2} \phi_m$):

$$\underline{V}_+ = \underline{V}_m \cdot \frac{\sqrt{2} \sin \zeta}{\beta} \cdot \frac{h\beta + j\underline{a}_2}{\underline{a}_1 + \underline{a}_2} \quad (9)$$

$$\underline{V}_- = \underline{V}_m \cdot \frac{\sqrt{2} \sin \zeta}{\beta} \cdot \frac{h\beta - j\underline{a}_1}{\underline{a}_1 + \underline{a}_2} \quad (10)$$

where:

$$\begin{aligned} h &= \frac{1 + \cos(\zeta)}{\sin(\zeta)} \\ \underline{a}_1 &= 1 - \frac{jX_c}{\underline{Z}_+} \cdot \left(1 + \frac{j}{\beta \cdot \tan(\zeta)} \right) \\ \underline{a}_2 &= 1 - \frac{jX_c}{\underline{Z}_-} \cdot \left(1 - \frac{j}{\beta \cdot \tan(\zeta)} \right) \end{aligned} \quad (11)$$

The presence of the capacitive impedance connected in series with the auxiliary winding requires a special usage of the symmetrical components. A suitable option is to include the capacitor voltage in the positive and negative sequence voltages. The positive and negative sequence impedances are approximated using the average of the apparent d and q axes impedances:

$$\underline{Z}_+ = R_s + jX_{ls} + \frac{1}{2} \cdot \left[\frac{jX_{md} \cdot \left(\frac{R_{rd}}{s} + jX_{lrd} \right)}{\frac{R_{rd}}{s} + j \cdot (X_{md} + X_{lrd})} + \frac{jX_{mq} \cdot \left(\frac{R_{rq}}{s} + jX_{lrq} \right)}{\frac{R_{rq}}{s} + j \cdot (X_{mq} + X_{lrq})} \right] \quad (12)$$

$$\underline{Z}_- = R_s + jX_{ls} + \frac{1}{2} \cdot \left[\frac{jX_{md} \cdot \left(\frac{R_{rd}}{2-s} + jX_{lrd} \right)}{\frac{R_{rd}}{2-s} + j \cdot (X_{md} + X_{lrd})} + \frac{jX_{mq} \cdot \left(\frac{R_{rq}}{2-s} + jX_{lrq} \right)}{\frac{R_{rq}}{2-s} + j \cdot (X_{mq} + X_{lrq})} \right] \quad (13)$$

Cage torque components

The following relations compute the average cage torque components (positive and negative sequence) valid for an m -phase AC motor with unbalanced stator voltage:

$$T_{(avg)+} = \frac{m}{2} \cdot \frac{P}{2} \cdot \operatorname{Re} \left\{ \left(\underline{\Psi}_{q+} \right)^* \underline{I}_{d+} - \left(\underline{\Psi}_{d+} \right)^* \underline{I}_{q+} \right\} \quad (14)$$

$$T_{(avg)-} = \frac{m}{2} \cdot \frac{P}{2} \cdot \operatorname{Re} \left\{ \left(\underline{\Psi}_{q-} \right)^* \underline{I}_{d-} - \left(\underline{\Psi}_{d-} \right)^* \underline{I}_{q-} \right\} \quad (15)$$

Each of these two average torque components can be further divided into another two components. This way, the analysis of the starting capabilities of the LSPM motor can be accomplished for a wider range of frequencies.

The electromagnetic asymmetry of the rotor leads to the following sequence components, as seen from the rotor reference frame:

I) For the positive sequence (sf), the rotor field is decomposed into two components: forward component, which rotates versus the rotor with sn_1 speed; backward component, which rotates versus the rotor with $(-sn_1)$ speed.

These two revolving fields rotate versus the stator with the following speed:

a) forward component:

$$sn_1 + n = sn_1 + (1-s)n_1 = n_1;$$

b) backward component:

$$-sn_1 + n = -sn_1 + (1-s)n_1 = (1-2s)n_1$$

II) For the negative sequence ($(2-s)f$), the rotor field is decomposed into two components: forward component, which rotates versus the rotor with $(2-s)n_1$ speed; backward component, which rotates versus the rotor with $(s-2)n_1$ speed. These two revolving fields, rotate versus the stator with the following speed:

a) forward component:

$$(2-s)n_1 + n = (2-s)n_1 + (1-s)n_1 = (3-2s)n_1;$$

b) backward component:

$$(s-2)n_1 + n = (s-2)n_1 + (1-s)n_1 = -n_1$$

The stator voltage equations (2) and (3) can be re-written as follows for the positive sequence components:

$$\begin{aligned} \underline{V}_+ &= R_s \underline{I}_{f+} + \frac{1}{2} \cdot (\underline{Z}_{d+} + \underline{Z}_{q+}) \underline{I}_{f+} + \frac{1}{2} \cdot (\underline{Z}_{d+} - \underline{Z}_{q+}) \underline{I}_{b+} \\ 0 &= \frac{R_s}{2s-1} \underline{I}_{b+} + \frac{1}{2} \cdot (\underline{Z}_{d+} - \underline{Z}_{q+}) \underline{I}_{f+} + \frac{1}{2} \cdot (\underline{Z}_{d+} + \underline{Z}_{q+}) \underline{I}_{b+} \end{aligned} \quad (16)$$

and respectively for the negative sequence component:

$$\begin{aligned} 0 &= \frac{R_s}{3-2s} \underline{I}_f + \frac{1}{2} \cdot (\underline{Z}_d + \underline{Z}_q) \underline{I}_f + \frac{1}{2} \cdot (\underline{Z}_d - \underline{Z}_q) \underline{I}_b \\ -\underline{V}_- &= R_s \underline{I}_b + \frac{1}{2} \cdot (\underline{Z}_d - \underline{Z}_q) \underline{I}_f + \frac{1}{2} \cdot (\underline{Z}_d + \underline{Z}_q) \underline{I}_b \end{aligned} \quad (17)$$

where the indices f, b stand for forward and backward components.

After algebraic manipulations we obtain the forward and backward current expressions as:

$$\underline{I}_{f+} = \underline{V}_+ \frac{\underline{Z}_{db+} + \underline{Z}_{qb+}}{\underline{Z}_{df+} \underline{Z}_{qb+} + \underline{Z}_{db+} \underline{Z}_{qf+}} \quad (18)$$

$$\underline{I}_{b+} = -\underline{V}_+ \frac{\underline{Z}_{df+} - \underline{Z}_{qf+}}{\underline{Z}_{df+} \underline{Z}_{qb+} + \underline{Z}_{db+} \underline{Z}_{qf+}} \quad (19)$$

$$\underline{I}_f = -\underline{V}_- \frac{\underline{Z}_{db-} - \underline{Z}_{qb-}}{\underline{Z}_{df-} \underline{Z}_{qb-} + \underline{Z}_{db-} \underline{Z}_{qf-}} \quad (20)$$

$$\underline{I}_b = \underline{V}_- \frac{\underline{Z}_{df-} + \underline{Z}_{qf-}}{\underline{Z}_{df-} \underline{Z}_{qb-} + \underline{Z}_{db-} \underline{Z}_{qf-}} \quad (21)$$

where:

$$\begin{cases} \underline{Z}_{d\pm} = jX_{d\pm} = \underline{Z}_{md\pm} + jX_{ls} \\ \underline{Z}_{q\pm} = jX_{q\pm} = \underline{Z}_{mq\pm} + jX_{ls} \end{cases} \quad (22)$$

$$\begin{cases} \underline{Z}_{df+} = \underline{Z}_{md+} + R_s + jX_{ls} \\ \underline{Z}_{qf+} = \underline{Z}_{mq+} + R_s + jX_{ls} \\ \underline{Z}_{db+} = \underline{Z}_{md+} + \frac{R_s}{2s-1} + jX_{ls} \\ \underline{Z}_{qb+} = \underline{Z}_{mq+} + \frac{R_s}{2s-1} + jX_{ls} \end{cases} \quad (23)$$

$$\begin{cases} \underline{Z}_{df-} = \underline{Z}_{md-} + \frac{R_s}{2s-3} + jX_{ls} \\ \underline{Z}_{qf-} = \underline{Z}_{mq-} + \frac{R_s}{2s-3} + jX_{ls} \\ \underline{Z}_{db-} = \underline{Z}_{md-} - R_s + jX_{ls} \\ \underline{Z}_{qb-} = \underline{Z}_{mq-} - R_s + jX_{ls} \end{cases} \quad (24)$$

The following relations compute the average cage torque components (positive and negative sequences split in forward and backward components) valid for an m -phase AC motor with unbalanced stator voltage:

$$T_{(avg)f+} = \frac{mP}{2\omega} \cdot R_{e+} \cdot |\underline{I}_{f+}|^2 \quad (25)$$

$$T_{(avg)b+} = \frac{mP}{2\omega} \cdot \frac{R_s}{2s-1} \cdot |\underline{I}_{b+}|^2 \quad (26)$$

$$T_{(avg)f-} = \frac{mP}{2\omega} \cdot \frac{R_s}{2s-3} \cdot |\underline{I}_{f-}|^2 \quad (27)$$

$$T_{(avg)b-} = \frac{mP}{2\omega} \cdot R_{e-} \cdot |\underline{I}_{b-}|^2 \quad (28)$$

where $R_{e(\pm)}$ represents the equivalent resistances computed with the following relations:

$$\begin{aligned} R_{e+} &= \operatorname{Re} \left\{ \frac{1}{2} \left[(\underline{Z}_{md+} + \underline{Z}_{mq+}) - \frac{(\underline{Z}_{md+} - \underline{Z}_{mq+})^2}{\underline{Z}_{db+} + \underline{Z}_{qb+}} \right] \right\} \\ R_{e-} &= \operatorname{Re} \left\{ \frac{1}{2} \left[-(\underline{Z}_{md-} + \underline{Z}_{mq-}) + \frac{(\underline{Z}_{md-} - \underline{Z}_{mq-})^2}{\underline{Z}_{df-} + \underline{Z}_{qf-}} \right] \right\} \end{aligned} \quad (29)$$

while the equivalent magnetization impedances are:

$$\begin{aligned} \underline{Z}_{md+} &= \frac{1}{\frac{1}{jX_{md}} + \frac{s}{R_{rd} + j \cdot sX_{lrd}}} \\ \underline{Z}_{mq+} &= \frac{1}{\frac{1}{jX_{mq}} + \frac{s}{R_{rq} + j \cdot sX_{lrq}}} \\ \underline{Z}_{md-} &= \frac{1}{\frac{1}{jX_{md}} + \frac{(2-s)}{R_{rd} + j \cdot (2-s)X_{lrd}}} \\ \underline{Z}_{mq-} &= \frac{1}{\frac{1}{jX_{mq}} + \frac{(2-s)}{R_{rq} + j \cdot (2-s)X_{lrq}}} \end{aligned} \quad (30)$$

The total average cage torque may be computed as:

$$T_{(avg)} = T_{(avg)+} + T_{(avg)-} = T_{(avg)f+} + T_{(avg)b+} + T_{(avg)f-} + T_{(avg)b-} \quad (31)$$

3. MODELLING THE MAGNET BRAKING TORQUE

A complete d-q axis analysis of the magnet braking torque for a 3-phase symmetrical LSPM motor is given in [2]. Expressions for determining the currents and the flux linkages due to the magnets, and the magnet braking torque are determined accordingly for the unsymmetrical single-phase LSPM motor:

$$\begin{cases} I_{dm} = \frac{-(1-s)^2 \cdot (X_q - X_c)}{R_s^2 + X_d (X_q - X_c) (1-s)^2} \cdot E_0 \\ I_{qm} = \frac{-(1-s) R_s}{R_s^2 + X_d (X_q - X_c) (1-s)^2} \cdot E_0 \end{cases} \quad (31)$$

$$\begin{cases} \Psi_{dm} = \frac{X_d I_{dm} + E_0}{\omega} \\ \Psi_{qm} = \frac{(X_q - X_c) \cdot I_{qm}}{\omega} \end{cases} \quad (32)$$

$$T_m = \frac{P}{2} \cdot \sin(\zeta) \left[\beta \cdot \Psi_{dm} I_{qm} - \frac{1}{\beta} \cdot \Psi_{qm} I_{dm} \right] \quad (33)$$

The expression (33) shows the possibility of decreasing the magnet braking torque when the stator windings of the single-phase LSPM motor are electrically non-orthogonal.

However, a more accurate analytical model may be needed for the magnet braking torque in the case of the 1-phase unbalanced LSPM motor, when the stator windings weight is not equal. The induced magnetic fluxes by the permanent magnet in both windings (main and auxiliary) depend on the rotor speed. Their amplitude is proportional to the effective ampere-turns in the respective winding. The magnet braking torque is given by the interaction between the stator currents and the induced magnetic fluxes by the permanent magnet in these windings. As the stator currents amplitude and phase angle are different, this explains why the exact analytical expression for this torque component is impossible to deduce, without several useful assumptions. A literature survey shows that even using the complicated FE technique, the magnet braking torque prediction has not yet been realised.

4. MODELLING THE PULSATING TORQUES

In a single-phase permanent magnet motor, several harmonic stator currents are present. These harmonic components are due to the asynchronous operation as an induction motor, and to the influence of the permanent magnets:

- the fundamental (f) represented by the positive forward and negative backward sequence cage component;
- $(1-2s)f$ harmonic, represented by the positive backward cage sequence;
- $(3-2s)f$ harmonic, represented by the negative forward cage component;
- $(1-s)f$ harmonic, represented by the induced stator currents due to the magnet rotation.

As the analysis of LSPM is made using a rotor reference frame, the stator harmonic current components correspond to two induced currents, and the equivalent current is determined by the permanent magnet. Their frequencies are: sf harmonic, represented by the positive cage sequence; $(2-s)f$ harmonic, represented by the negative cage sequence; 0, represented by the permanent magnet equivalent current.

These harmonics interact and determine several pulsating torques: four cage pulsating torque components and two permanent pulsating torque components. Table I shows the interaction between harmonic rotor currents, and the resultant pulsating torque frequencies.

TABLE I. HARMONICS OF THE PULSATING TORQUE

Frequency components	Positive seq. sf	Negative seq. $(2-s)f$	Magnet 0
Positive seq. sf	$2sf$	$2f, (2-2s)f$	sf
Negative seq. $(2-s)f$	$2f, (2-2s)f$	$(4-2s)f$	$(2-s)f$
Magnet 0	sf	$(2-s)f$	0

We may classify the amplitude (zero to peak) of the pulsating torques according to their main cause in: reluctance, unbalanced stator and permanent magnet (excitation) pulsating torque components.

Reluctance pulsating torques

$$T_{(\text{puls})(2sf)} = \frac{m}{2} \cdot \frac{P}{2} \cdot \text{Abs} \left\{ \left(\underline{\psi}_{q+} \right) \underline{I}_{d+} - \left(\underline{\psi}_{d+} \right) \underline{I}_{q+} \right\} \quad (34)$$

$$T_{(\text{puls})(4-2s)f} = \frac{m}{2} \cdot \frac{P}{2} \cdot \text{Abs} \left\{ \left(\underline{\psi}_{q-} \right) \underline{I}_{d-} - \left(\underline{\psi}_{d-} \right) \underline{I}_{q-} \right\} \quad (35)$$

Unbalanced stator pulsating torques

$$T_{(\text{puls})(2f)} = \frac{m}{2} \cdot \frac{P}{2} \cdot \text{Abs} \left\{ \left(\underline{\psi}_{q+} \right) \underline{I}_{d-} - \left(\underline{\psi}_{d+} \right) \underline{I}_{q+} \right\} \quad (36)$$

$$T_{(\text{puls})(2-2s)f} = \frac{m}{2} \cdot \frac{P}{2} \cdot \text{Abs} \left\{ \left(\underline{\psi}_{q-} \right) \underline{I}_{d+} - \left(\underline{\psi}_{d-} \right) \underline{I}_{q-} \right\} \quad (37)$$

Permanent magnet (excitation) pulsating torques

$$T_{(\text{puls})(sf)} = m \cdot \frac{P}{2} \cdot \text{Abs} \left\{ \left[\left(\underline{\psi}_{q+} \right) \underline{I}_{dm} + \left(\underline{\psi}_{qm} \right) \underline{I}_{d+} \right] - \left[\left(\underline{\psi}_{d+} \right) \underline{I}_{qm} + \left(\underline{\psi}_{dm} \right) \underline{I}_{q+} \right] \right\} \quad (38)$$

$$T_{(\text{puls})(2-s)f} = m \cdot \frac{P}{2} \cdot \text{Abs} \left\{ \left[\left(\underline{\psi}_{q-} \right) \underline{I}_{dm} + \left(\underline{\psi}_{qm} \right) \underline{I}_{d-} \right] - \left[\left(\underline{\psi}_{d-} \right) \underline{I}_{qm} + \left(\underline{\psi}_{dm} \right) \underline{I}_{q-} \right] \right\} \quad (39)$$

Note that while the reluctance and excitation pulsating torques total effect is given by their sum, the unbalanced stator pulsating torque effect is given by their difference.

5. EXPERIMENTAL AND SIMULATION RESULTS

The experiments were performed on three motor types, equipped with identical rotor, and stator lamination, but with different stator windings. Note that the assumption made in section II, is not valid. This way it is possible to observe the influence of this simplification on the simulations, when compared to the experimental data.

TABLE II. STATOR WINDING DATA

Motor Type	Winding parameters			
	N_m [p.u.]	β	ϕ_m / ϕ_a	ζ [elec. °]
Motor A	1.46	1.42	1.22	90
Motor B	1.14	1.42	1.3	90
Motor C	1	1	1	90
Motor D	0.87	0.70	0.76	90

During starting, the accelerating torque of LSPM motor is the average cage torque minus the magnet braking torque and the load torque. The average cage torque is developed by "induction motor action", except that the saliency and the unbalanced stator voltages complicate the analysis and may compromise the performance.

The magnet braking torque is produced by the fact that the magnet flux generates currents in the stator windings, and is associated with the loss in the stator circuit resistance. The variation of this torque with speed follows a pattern similar to

that in the induction motor, but the per-unit speed takes the place of the slip.

The magnet braking torque should not be confused with the synchronous “alignment” torque that arises at synchronous speed, even through the magnet braking torque is still present at synchronous speed and therefore diminishes the output and the efficiency. The magnet alignment torque has a non-zero average value (i.e., averaged over one revolution or electrical cycle) only at synchronous speed. At all other speeds it contributes an oscillatory component of torque that is very evident in Figs. 11-13. The same is true of the reluctance torque. As the rotor approaches synchronous speed, the screening effect of the cage becomes less, and as the slip is very small, the oscillatory synchronous torques (alignment and reluctance) cause large variations in speed that may impair the ability to synchronize large-inertia loads. There are presented the simulation results for the case when two capacitors are used, 23 μF at low speed and 3 μF at high speed (above 80-90% of synchronous speed), for all the analysed LSPM motor types. Note that these values do not correspond to the optimum values of any of the analysed motors. A trade-off has to be made depending on the application: lower starting torque and efficiency, but increased load torque and synchronization capability (motor B); higher starting torque and efficiency, but decreased load torque and synchronization capability (motor A and C); higher starting and load torque and synchronization capability, but lower efficiency and higher magnetic noise i.e., pulsating torques (motor D).

The magnet braking torque exhibits a maximum in a range from 0.25 Nm (Motor B) to 0.65 Nm (Motor D). The cage torque in all the cases overcomes the magnet braking torque.

Figs. 2-5 illustrate the experimental quasi steady-state torque variation vs. speed during no-load operation for a line-start permanent magnet motor, supplied with an unbalanced stator voltage system, with a capacitor-start value 23 μF . The higher torque values have been measured when the rotor is without permanent magnets (T_{avg}). The lower torque values represent the experimental data for the real motor equipped with permanent magnets ($T_{\text{avg}} + T_m$). The capacitor value was not optimised, as the experiments were intended to study the torque behaviour during starting operation, for a wide range of capacitance values.

Figs. 6-9 present the average torque components, in quasi steady-state analysis. The solid line represents the resultant average torque, while the dotted lines show the cage torque components and dashed line shows magnet braking torque. A comparison with the experimental results in Figs. 2-5 shows an overall good agreement for motors B and C, while for motor A the predictions are accurate for low and high speed (slip belongs to intervals [0, 0.3] and [0.85, 1]).

Figs. 10-13 show the pulsating torque components zero to peak amplitude. The solid lines represent the cage pulsating torque components, while the magnet pulsating torque components are illustrated using dashed lines. One can note the higher values for the unbalanced stator (eqs. 34, 35) and magnet (excitation) pulsating torque (eqs. 38, 39).

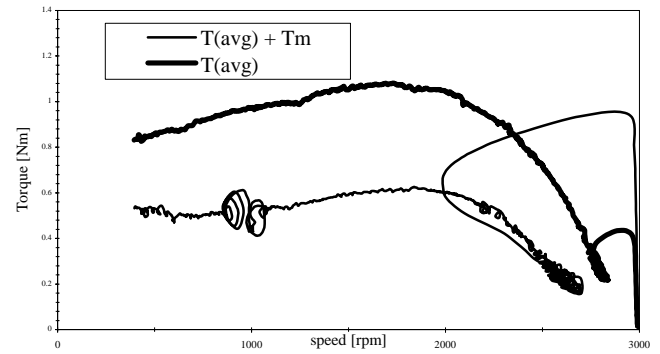


Fig.2 Experimental torque variation vs. speed during no-load operation, Motor A

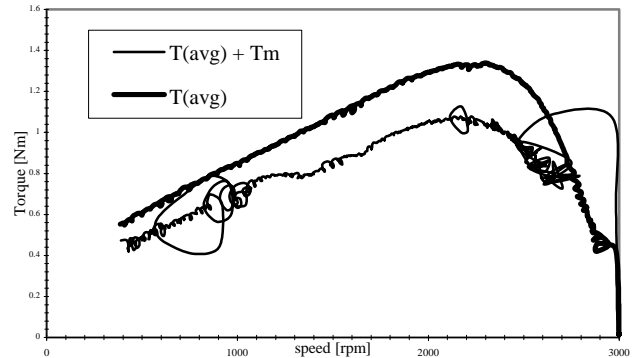


Fig.3 Experimental torque variation vs. speed during no-load operation, Motor B

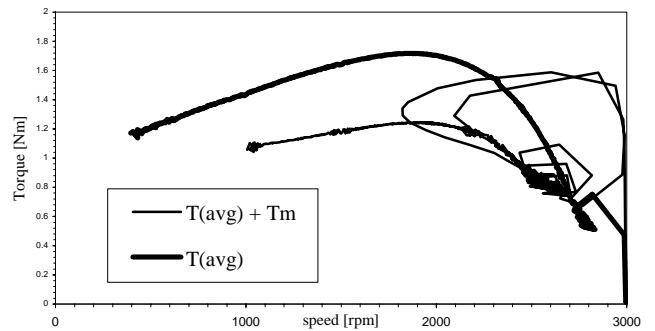


Fig.4 Experimental torque variation vs. speed during no-load operation, Motor C

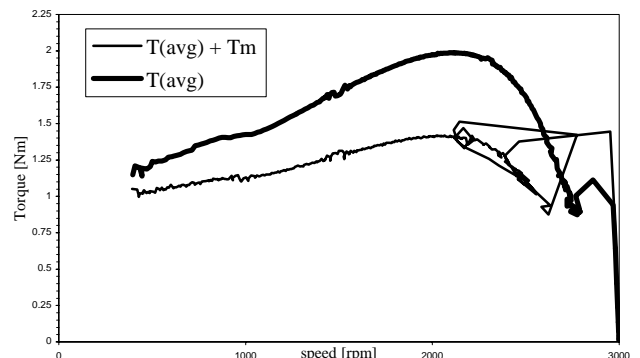


Fig.5 Experimental torque variation vs. speed during no-load operation, Motor D

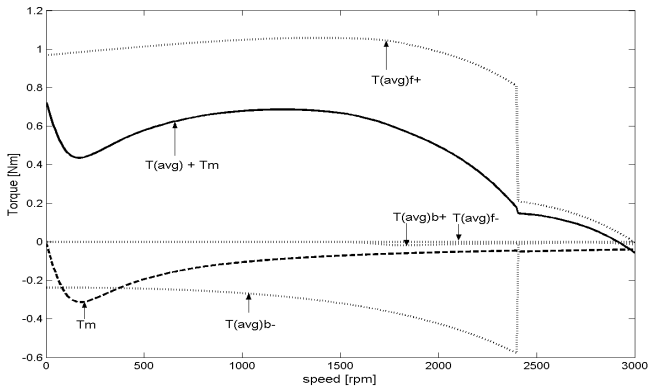


Fig. 6 Resultant torque components (cage and magnet braking torque) variation vs. speed during starting operation – Motor A

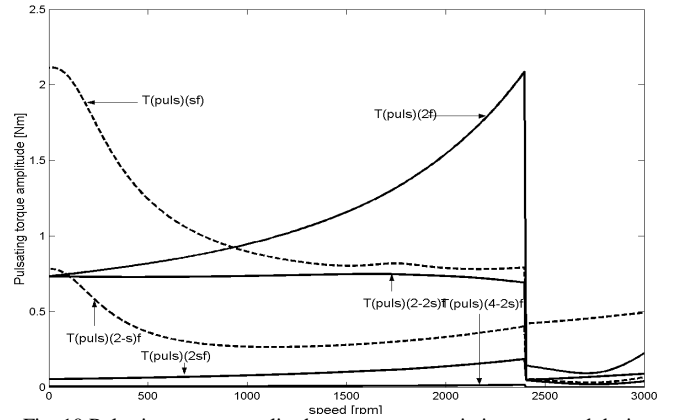


Fig. 10 Pulsating torque amplitude components variation vs. speed during starting operation – Motor A

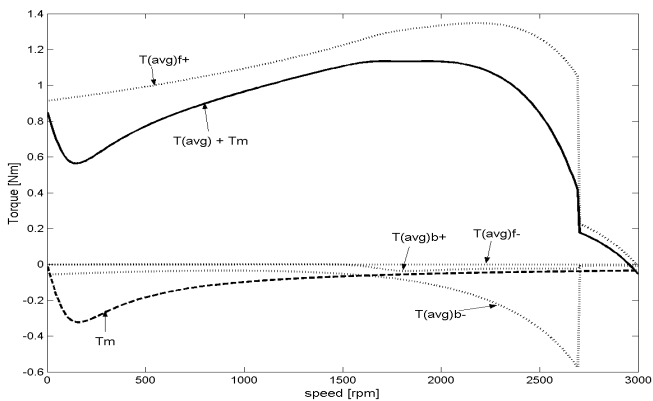


Fig. 7 Resultant torque components (cage and magnet braking torque) variation vs. speed during starting operation – Motor B

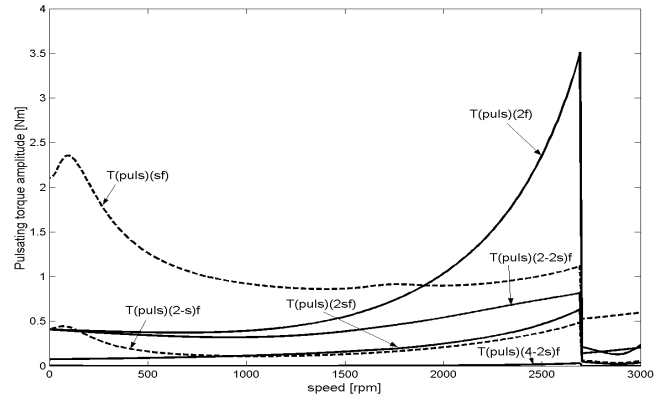


Fig. 11 Pulsating torque amplitude components variation vs. speed during starting operation – Motor B

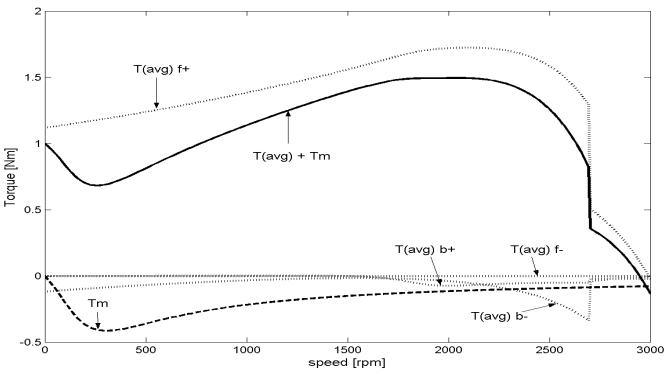


Fig. 8 Resultant torque components (cage and magnet braking torque) variation vs. speed during starting operation – Motor C

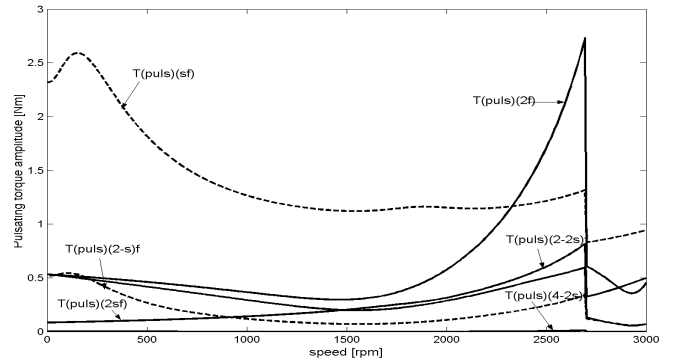


Fig. 12 Pulsating torque amplitude components variation vs. speed during starting operation – Motor C

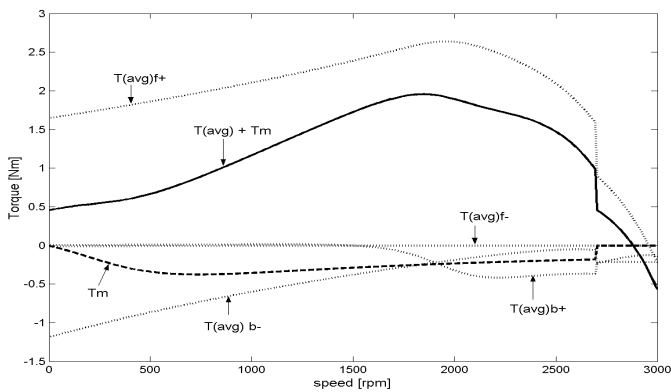


Fig. 9 Resultant torque components (cage and magnet braking torque) variation vs. speed during starting operation – Motor D

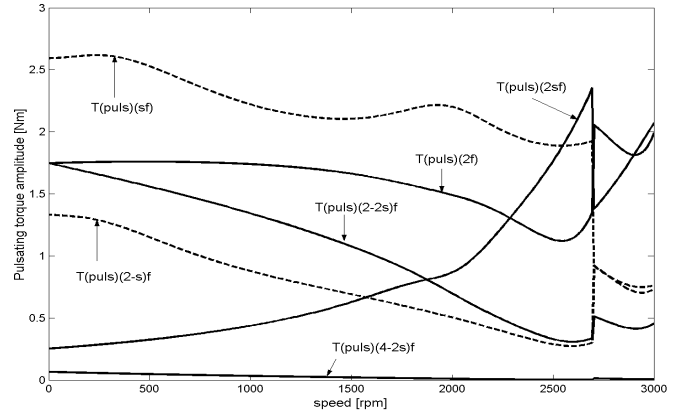


Fig. 13 Pulsating torque amplitude components variation vs. speed during starting operation – Motor D

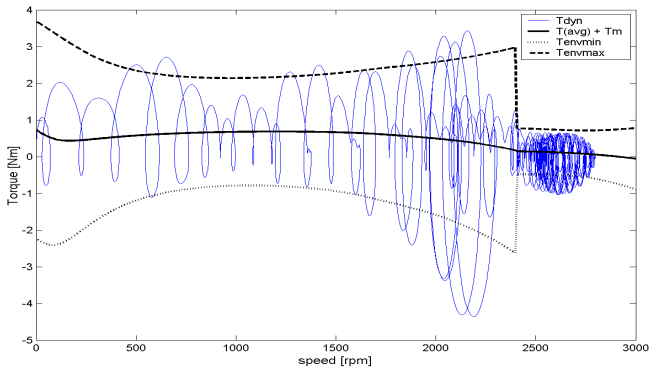


Fig. 14 Dynamic, resultant torque and envelope with pulsating components variation vs. speed during starting operation – Motor A

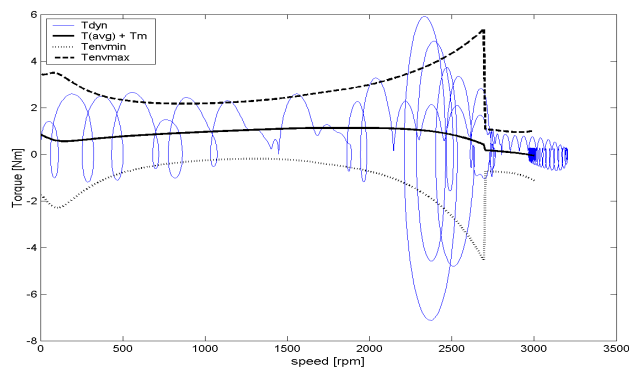


Fig. 15 Dynamic, resultant torque and envelope with pulsating components variation vs. speed during starting operation – Motor B

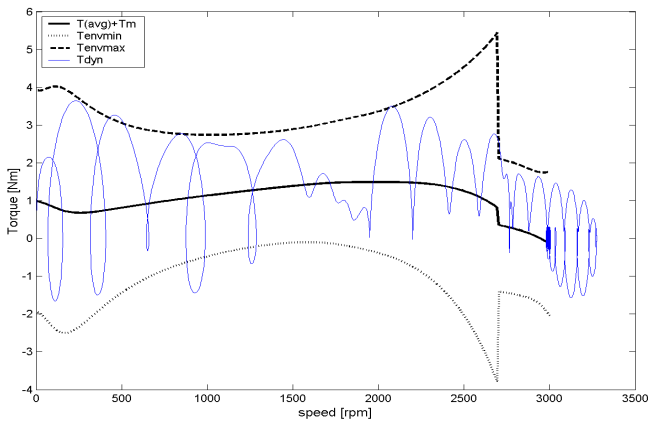


Fig. 16 Dynamic, resultant torque and envelope with pulsating components variation vs. speed during starting operation – Motor C

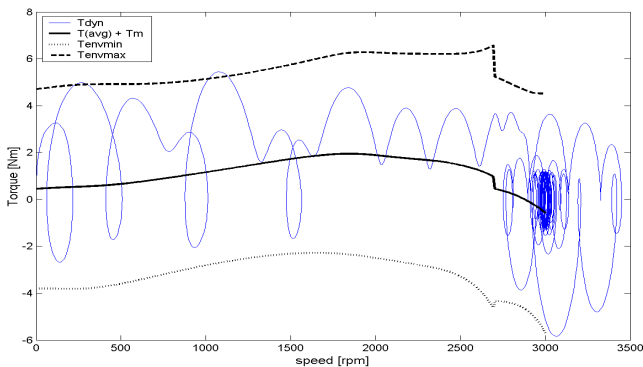


Fig. 17 Dynamic, resultant torque and envelope with pulsating components variation vs. speed during starting operation – Motor D

In Figs. 14-17, the dynamic torque and quasi-steady state average resultant torque (solid line) and the envelope of the instantaneous torque are presented (dashed lines). The dynamic torque simulation pattern follows that described in [1]. The minimum and maximum envelope trajectory (T_{envmax} , T_{envmin}) are obtained by superimposing the pulsating torque components effect over the average resultant torque. This approach neglects the mechanical pulsation due to rotor/load inertia and assumes that even though pulsating torque components vary with different frequencies, their global effect may be simulated by superposition. The slight difference between the quasi steady-state torque and dynamic torque is due to the rotor inertia influence and the pulsating torque variation with frequency harmonics (Table I).

All simulations have been implemented neglecting saturation and core losses. However, the proposed model equations may include any non-linearity effect.

The equivalent circuit parameters defined in the Appendix have been either measured or computed with the use of *SPEED*[®] software: *PC-IMD v. 3.0*, *PC-BDC v.6.0* and *PC-FEA v. 5.0*.

6. TORQUE COMPONENTS CHARACTERISTICS

For the average *cage torque components*, the main observations are:

I) The positive forward sequence torque ($T_{(avg)f+}$) is the main component, which ensures good starting capabilities for a single-phase permanent magnet motor. The starting capabilities require a high-resistance rotor cage, but this feature will present the classical “dip” at half synchronous speed, in a similar way to the Goerges [4] phenomenon in induction motors with an unsymmetrical rotor. This “dip” can be minimised by using lower resistance rotor bars, or almost symmetrical cage rotors, i.e. $R_{rd} \approx R_{rq}$. Therefore, an optimum value for the cage rotor resistance must be employed.

II) The positive backward sequence torque ($T_{(avg)b+}$) which amplifies the half synchronous speed “dip”, and the negative forward sequence torque ($T_{(avg)f-}$) which always has negative values and diminishes the resultant cage torque, can be minimised by using a minimum admissible value for the stator resistance. However, this task is hard to achieve for small motors ($P_n < 1kW$).

III) Obviously, the minimisation of negative sequence voltage amplitude toward zero (i.e. by using a correct choice for the run capacitor [1]), leads to the elimination of negative sequence average torque components.

IV) It is of interest that the developed airgap cage torque at synchronous speed is not zero as in a symmetrical induction motor. The cage torque of the asymmetrical PM machine at $s = 0$ is always *negative*, because of the negative forward sequence torque ($T_{(avg)f-}$), except when $X_d = X_q$, where the stator windings are identical and the cage torque becomes zero (i.e. case of a 2-phase balanced induction motor).

For the *magnet braking torque*, the main observations are:

I) The maximum amplitude of the magnet braking torque may be decreased by employing a suitable value for the stator windings shift angle (ζ) [10], or an over unit value for turns ratio (β).

II) The corresponding speed for the maximum amplitude of the magnet braking torque is susceptible to occur at higher than half synchronous speed for 1-phase unsymmetrical LSPM motor.

III) For pure single-phase motors (split-phase), when only one stator winding is energized, the magnetic field created by excitation (permanent magnets) transforms from a revolving field into a pulsating field and the corresponding braking torque vanishes.

For the *pulsating torque components*, the main observations are:

I) The asymmetries on both stator and rotor determines six important pulsating torque components for the run-up period [$2sf$, $2f$, $(2-2s)f$, $(4-2s)f$, $(2-s)f$, sf] and two components for the synchronous operation [$2f$, $4f$], compared to two and zero components respectively for the 3-phase symmetrical motor case [2].

II) All six pulsating torque components for the run-up period can further be split into another two components, if the analysis is to be made from the stator point of view.

III) Even for a symmetrical rotor (i.e. d-q axis parameters are identical), the pulsating excitation and unbalanced stator torque components will not disappear completely. The unsymmetrical stator pulsating torque components ($2f$ and $(2-2s)f$) are always present for an unbalanced stator voltage system. The double frequency pulsating torque component represents the main cause of pulsating for the single-phase LSPM motor. This component is characteristic for any 1-phase AC motor: induction, synchronous reluctance, or synchronous permanent magnet.

IV) The forward sequence excitation pulsating component (eq. 38) is responsible for larger pulsations especially at low speed (slip $\cong 1$), whilst the negative sequence excitation pulsating component (eq. 39) has a comparable value with the reluctance pulsating torque components (eqs. 34, 35).

V) The reluctance pulsating torque components [$2sf$ and $(4-2s)f$] are entirely dependent on the machine parameters (resistances and reactances). The difference between rotor d-q axis resistances and leakage reactances ($R_{rd} \neq R_{rq}$, $X_{lrd} \neq X_{lrq}$) determines an increased pulsating “dip” torque around the half synchronous speed region. The difference between magnetisation d-q axis reactances ($X_{md} \neq X_{mq}$) determines an increased pulsating torque around the synchronous speed region.

VI) The rotor asymmetry is responsible for the non-zero reluctance pulsating torque at standstill ($s = 1$), and the stator asymmetry is responsible for the non-zero unbalanced stator pulsating torque even at synchronous speed operation. For a single-phase permanent magnet motor, the proper selection of a capacitor to obtain a balanced stator voltage system will lead only to the minimisation toward zero of the stator asymmetry effect. The rotor asymmetry effect cannot be eliminated.

7. CONCLUSIONS

The asynchronous performance prediction for a line start permanent magnet motor can be made using a quasi steady-state analysis. Important information about the motor torque capability is obtained through the study of different torque

components. The deduced torque expressions are valid for the general case of the m -phase AC motor, supplied with unbalanced stator voltage.

REFERENCES

- [1]. Miller, T.J.E. “Single-phase permanent magnet motor analysis”, *IEEE Trans. Ind. Appl.*, Vol. IA-21, pp. 651-658, May-June 1985
- [2]. Honsinger, V.B. “Permanent magnet machine: Asynchronous operation”, *IEEE Trans. Power Appl. Syst.*, vol. PAS-99, pp.1503-1509, July 1980
- [3]. Adkins, B., Harley, R.G. *The general theory of alternating current machines*, Chapman & Hall, 1975
- [4]. Boldea, I., Dumitrescu, T., Nasar, S. “Unified analysis of 1-phase AC motors having capacitors in auxiliary windings” *IEEE Transactions on En. Conv.*, Vol. 14, No.3, pp. 577-582, September 1999
- [5]. Gabarino, H.L., Gross, E.T.B. “The Goerges phenomenon – induction motors with unbalanced rotor impedances” *AIEE Trans.*, Vol. 69, pp.1569-1575, 1950
- [6]. Williamson, S.; Knight, A.M. “Performance of skewed single-phase line-start permanent magnet motors” *IEEE Transactions on Ind. Appl.*, Vol. 35, pp. 577 –582, May-June 1999
- [7]. Stephens, C.M.; Kliman, G.B.; Boyd, J. “A line-start permanent magnet motor with gentle starting behavior” *IEEE Industry Applications Conference, 1998*, Vol. 1, pp. 371 –379, 1998
- [8]. Rahman, M.A.; Osheiba, A.M. “Performance of large line-start permanent magnet synchronous motors”, *IEEE Transactions on En. Conv.*, Vol. 5, pp. 211-217, March 1990
- [9]. Carlson, R. , Sadowski, N., Arruda, S. R., da Silva, C. A., Von Dokonal, L. “Single-phase line-started permanent magnet motor analysis using finite element method” *IEEE Industry Applications Conference, 1994*, Vol.1, pp: 227 –233
- [10]. Popescu, M., Jokinen, T., Demeter, E., Navrapescu, V.- “Modelling and analysis of a two-phase induction machine with non-orthogonal stator windings” – in *Conf. Rec. IEEE IEMDC’99*, May 1999, Seattle, USA, pp.389-391

APPENDIX

List of symbols

\underline{V}_m – complex main supply voltage

$\underline{V}_{+,-}$, $\underline{Z}_{+,-}$ – complex positive/negative sequence voltage and impedance

$\underline{V}_{d,q}$, $\underline{I}_{d,q}$ – complex d-q axis voltage/current components in rotor reference frame

R_s, R_a, R_m – stator winding resistance: equivalent/auxiliary/main

X_{ls}, X_{la}, X_{lm} – stator leakage reactance: equivalent/auxiliary/main

β, ζ - turns ratio (main/aux) and shift electrical angle between stator windings

R_{rd}, R_{rq} – rotor resistance for d-q axis

X_{lrd}, X_{lrq} – rotor leakage reactance for d-q axis

X_{md}, X_{mq} - magnetization reactance for d-q axis

$\underline{X}_{d\pm}, \underline{X}_{q\pm}$ – complex positive/negative asynchronous reactance for d-q axis

X_d, X_q - synchronous reactance for d-q axis

X_C, C_{run} – capacitive impedance/run capacitor value

m, P – phases and poles number

ω, s - synchronous speed [rad/sec] and slip

E_0 – no-load induced voltage

N_m – number of turns on main stator winding

$\phi_{m,a}$ – diameter of the main/auxiliary winding